

Transport in disordered graphene nanoribbons

Ivar Martin¹ and Ya. M. Blanter^{2,3}

¹*Theoretical Division, Los Alamos National Laboratory, Los Alamos, New Mexico, 87544, USA*

²*Kavli Institute of Nanoscience, Delft University of Technology, Lorentzweg 1, 2628 CJ Delft, The Netherlands*

³*Centre for Advanced Study, Drammensveien 78, 0271 Oslo, Norway*

(Dated: December 30, 2021)

We study electronic transport in graphene nanoribbons with rough edges. We first consider a model of weak disorder that corresponds to an armchair ribbon whose width randomly changes by a single unit cell size. We find that in this case, the low-temperature conductivity is governed by an effective one-dimensional hopping between segments of distinct band structure. We then provide numerical evidence and qualitative arguments that similar behavior also occurs in the limit of strong uncorrelated boundary disorder.

I. INTRODUCTION

Since the invention of the method for production graphene¹, many creative ideas for physical effects and devices have been put forth². Whereas early papers emphasized unusual electron properties of graphene as compared with ordinary metallic and semiconductor materials, it had been soon realized that graphene is a promising material for implementation of previously known physical devices with considerably improved characteristics. One of possible applications would be in semiconductor technology: excellent mechanical properties, easily tunable electron concentration, zero nuclear spin, and simple production are among the advantages that make graphene a much sought after material. However, the drawback preventing the use of graphene for semiconducting applications is exactly what is usually considered to be its main feature — the absence of a gap in the spectrum. In the absence of the gap, it is impossible to make even the simplest conventional electronic devices. For instance, a graphene p-n junction does not rectify current, even though it has some other interesting properties due to the Klein tunneling³. Similarly, hybrid graphene – normal metal systems are conducting for arbitrary gate voltage applied to graphene⁴. The only known way to open a gap in monolayer graphene is to use confined geometries — graphene quantum dots⁵ and graphene nanoribbons (GNR).

The electronic structure of ideal GNR is theoretically well established. It is very sensitive to the ribbon geometry, *i.e.* orientation relative to the crystal axes and their exact width^{6,7,8,9}. Within a tight-binding model with only nearest neighbor hopping, GNR with zig-zag edges have flat near-zero-energy bands of extended edge states, while ribbons with armchair edges, depending on the precise width, can be either metallic or semiconducting with the gap inversely proportional to the GNR width. Numerical studies¹⁰ show that passivation of the edges of ideal GNR — chemical bonding of edge carbon atoms with hydrogen — may open a small energy gap that does not scale with the GNR width.

Recently, first experimental observations of transport in GNR have been reported^{11,12,13,14,15}. GNR with

widths in the range from about 10 nm to 100 nm and lengths in the micrometer range have been studied. The fabrication procedure does not yet allow to control the GNR width with atomic precision (although chemical fabrication¹³ may eventually yield controlled edge fabrication). As a result the edges are disordered on the atomic length scale, as well as show longer-range width variation of a few nanometers. For narrow enough ribbons ($\lesssim 50$ nm) an unambiguous signature of the *geometric* gap E_g scaling with the inverse *average* ribbon width has been extracted from the gate voltage and temperature dependencies of conductivity^{11,12}. In particular, in Ref. 11, in a broad range of temperatures, T , conductivity scales as $e^{-E_g/T}$. The measured gap is a smooth function of the ribbon width, and is insensitive to the GNR orientation relative to the crystal axes. Also, $1/f$ current noise has been observed at low frequencies, $f < 100$ Hz, with the intensity proportional to the GNR width¹¹.

These experimental results are definitely inconsistent with the theory for ideal GNR that predicts different behavior depending on the orientation, typically with many low-energy states. The observed effects are clearly due to disorder. Indeed, it is natural to expect that any disorder, bulk or boundary, should lead to Anderson localization and open a transport gap; however, one would expect that this gap should be defined by the strength of disorder, rather than by the GNR width.

In this work we provide a qualitative resolution to this apparent puzzle by showing that electronic properties of the disordered GNR are indeed very different from the clean GNR. We demonstrate that for the states near the middle of the band, edge disorder leads to *segmentation* of the wavefunctions into blocks of length of the order of GNR width. Thus, at low temperatures, the system maps onto an effective one-dimensional (1D) hopping insulator¹⁶. We illustrate this behavior first with a model where disorder is introduced through slowly fluctuating ribbon width, which allows more direct numerical and analytical analysis (Section II). Then we generalize the results to the experimentally relevant case of strong disorder (Section III). Discussion and conclusions are presented in Section IV).

II. WEAK DISORDER

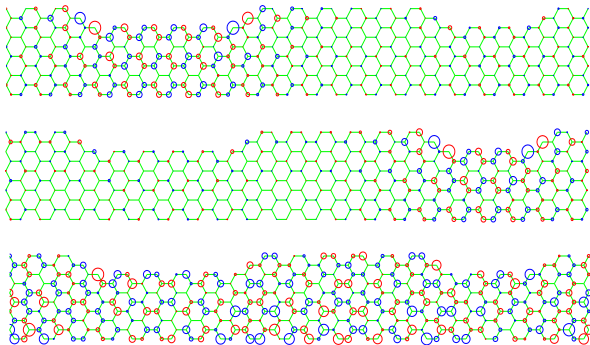


FIG. 1: Structure of the electronic wavefunctions in a “weakly disordered” armchair GNR. Periodic boundary conditions are applied in the horizontal direction. In our convention, the narrow segments have width $W = 4\sqrt{3}$, and in the limit of infinite length would have no band gap; the surrounding regions (width $W = 5\sqrt{3}$) for an infinitely long ribbon would have a gap $E_g = 2 \times 0.169t$ around zero energy (the middle of the GNR π band). The radii of the circles are proportional to the site amplitudes of the wavefunction, with the color representing sign. The top plot corresponds to a the lowest energy state inside the gap, $E = -0.096t$, spatially localized in the left (longer) metallic segment; the middle – to the low energy state in the right (shorter) metallic segment, $E = -0.131t$; the bottom is a delocalized state well outside the gap, $E = -0.497t$. Note the abrupt change in the localized wavefunctions’ amplitude at the “interface,” and rather uniform amplitude across the ribbon.

Let us consider an armchair GNR. An ideal ribbon of the width W , measured in units of minimal carbon-carbon distance, a_g , is metallic (no gap) for $W = (3N + 1)\sqrt{3}$, and semiconducting (with gap $E_g \sim t/W$) for $W = 3\sqrt{3}N$ and $W = (3N + 2)\sqrt{3}$, Ref. 9. Here, t is the graphene nearest-neighbor hopping matrix element (we neglect the next-nearest neighbor hopping which causes slight particle-hole asymmetry), and N is an integer. *Weak disorder* can be introduced as geometric fluctuations of the ribbon width, such that the “disordered” ribbon is comprised of ideal segments of random length of order L , with width changing from segment to segment. We assume that $L > W$. An example of a “disordered” configuration of this kind is shown in Fig. 1. While this situation has not been yet realized experimentally, it has the advantage that its analysis is straightforward, and, as we will argue, the behavior is related to the experimentally relevant case of strong disorder. If the length of each segment is longer than its width, to the lowest order, one can consider individual band structure of each segment separately. Depending on the width, some of the segments are nearly metallic, with the finite size gap of about t/L , while others are “insulating” with the gap t/W . In Fig. 1 we show the results of numerical diagonalization of the tight-binding graphene Hamiltonian — representative wavefunctions in different regions.

Note that although the segmentation is caused by the surface defect (change of the width by just one row of atoms!), the wavefunctions show high degree of uniformity *across* the ribbon, and rather sharp confinement to the respective regions *along* the ribbon. Thus, at low energies ($|E| < t/W$) it is natural to represent the system by a one-dimensional hopping model,

$$H = \sum_{i\alpha} \epsilon_i^\alpha \hat{c}_i^{\alpha\dagger} \hat{c}_i^\alpha + \sum_{i\alpha,j\beta} t_{ij}^{\alpha\beta} \hat{c}_i^{\alpha\dagger} \hat{c}_j^\beta + h.c. . \quad (1)$$

Here, the operator $\hat{c}_i^{\alpha\dagger}$ (\hat{c}_i^α) creates (destroys) electron in the metallic “grain” i in the orbital α .

To complete the formulation of the effective model Eq. (1) we need to determine the distributions of the on-site energies ϵ_i^α and inter-site hopping matrix elements $t_{ij}^{\alpha\beta}$. For simplicity we assume that the average length of the segments, both insulating and metallic, is the same, L_{av} . The low-energy spectrum in the metallic segments follows from the Dirac dispersion of the infinite metallic armchair GNR⁹, $\epsilon = c|k|$, where $c = 3ta_g/2$ and k is the momentum along GNR. The levels in a given metallic segment of length L are therefore approximately equidistant, with the average level spacing $\sim t/L$. In Figure 2 we show the result of a tight-binding calculation for the lowest energy state as a function of the length of a metallic segment embedded in the insulating GNR. Indeed we find that the energy scales approximately as $1/L$. Even better fit is obtained by using the form $1/(L + L_W)$ which takes into account the leakage of the wavefunction from the metallic regions into surrounding insulating ones. Note that $L_W \approx W$. If the lengths L_i for all grains were equal, the level structures in all grains would be identical (apart from the small splitting caused by inter-grain tunneling). However, for a distribution of lengths, the energy levels in different grains are likely to be out of registry by the amount $\sim t/L_{av}$.

We now evaluate the tunneling matrix elements t_{ij} between low-energy states in metallic segments. Tunneling occurs through the intermediate states in the insulating regions. The states just outside the gap are particularly important for tunneling. Near the gap edge the dispersion is quadratic, $\epsilon = \sqrt{c^2k^2 + (E_g/2)^2} \approx E_g/2 + c^2k^2/E_g$. This corresponds to the effective mass in the insulating regions $m^* \sim (Wa_g^2t)^{-1}$. The tunneling amplitude through a barrier of height E_g and length D can be estimated using the WKB approximation as $e^{-\alpha D/W}$, where α is a numerical coefficient of order 1. We have also verified this by a direct tight-binding calculation of the tunnel splitting of energy levels in two identical metallic segments separated by an insulating segment of variable length.

From the distributions of ϵ_i^α and $t_{ij}^{\alpha\beta}$, it follows that for $L_{av} > W$, the level spacing in the metallic grains is larger than the tunneling amplitude between the neighbors, making it impossible to have metallic, i.e. band, conduction. The system is a one-dimensional example of a simple impurity band insulator, a standard model used

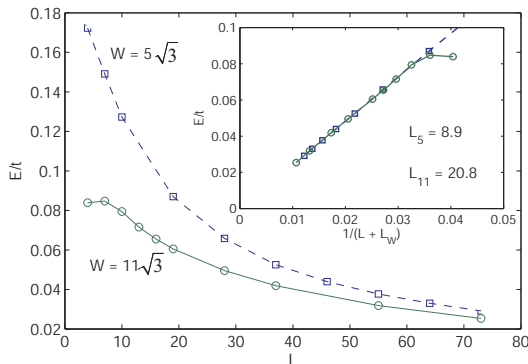


FIG. 2: The lowest energy state in a GNR as a function of length L of a “metallic” constriction surrounded by an “insulator.” The configuration is similar to the one in Fig. 1. The total length of the ribbon used in simulation is $120a_g$ (with periodic boundary conditions along horizontal axis). The results presented are for two GNR widths, $W = 5\sqrt{3}$ and $W = 11\sqrt{3}$, with $W = 4\sqrt{3}$ and $W = 10\sqrt{3}$, respectively, in the metallic regions. In the inset we fit the energy to the form $E \propto (L + L_W)^{-1}$. The offset L_W appears due to the leakage of the wavefunction from the metallic regions into the insulating ones. As expected (see text), $L_W \sim W$.

to describe lightly doped compensated semiconductors¹⁷. The finite-temperature conductivity of such insulator can be evaluated by standard techniques¹⁶,

$$\sigma \sim e^{-\alpha n L_{av}/W - t/(n L_{av} T)}, \quad (2)$$

where T is the temperature, and n is the length of the optimal jump. By minimizing the exponent, we find that $n_{opt} = \sqrt{tW/(\alpha L_{av}^2 T)}$. Hence there is a crossover from the nearest neighbor ($n_{opt} = 1$, NNH) to variable range hopping ($n_{opt} > 1$, VRH) at temperature $T^* \sim tW/L_{av}^2$,

$$\sigma \sim \begin{cases} e^{-2\sqrt{\alpha t/(WT)}} & \text{for } T < T^* \\ e^{-\alpha L_{av}/W - t/(L_{av} T)} & \text{for } T^* < T < t/L_{av} \end{cases} \quad (3)$$

Note that $T^* < t/W$, and thus both behaviors are possible within our model. At temperatures higher than t/L_{av} multiple states in the metallic regions have to be included. We do not consider here other regimes of one-dimensional hopping¹⁸ that can become relevant at very low temperatures.

III. STRONG DISORDER

We now turn to the *strong* disorder case, when the boundary is randomized at the atomic scale (this models the situation when some atoms are cut out or replaced by other atoms, e.g. oxygens, in the process of fabrication). Yet, we assume that the relative variation of the ribbon width introduced by disorder is small. This is different from the near-granular case considered in Ref. 19.

An example of a “strongly” disordered configuration that corresponds to small relative variation in the rib-

bon width is shown in Fig. 3. We chose a perfect zig-zag nanoribbon as the reference structure. Ideal zig-zag nanoribbons are always metallic, for any ribbon width, due to the presence of the edge states⁶. We observe that edge disorder (here generated by eliminating at random half of the sites along the edges) leads to the wavefunction localization. However, since disorder is now short-correlated, the wavefunctions no longer have a typical extent along the ribbon, but rather can be either more or less localized. We find numerically that the wavefunctions corresponding to the low-energy states ($|E| < t/W$) that are highly localized along the direction of the boundary ($L \ll W$, e.g. Fig. 3a) also do not penetrate deep inside the ribbon, having large amplitude only near the surface. On the other hand, states that are more extended along the ribbon also penetrate deeper into the bulk. This effect can be traced back to the behavior of the edge states in zig-zag GNR – the wavevector along the ribbon for these states is approximately equal to their exponential decay length into the bulk. In effect, in the absence of next-nearest-neighbor hopping, one can have states with very low energy, $\sim te^{-W/a}$, localized over the distance of about single unit cell near the ribbon edge. The number of such states within a segment of length W can be easily estimated to be $|K - K'|/(2\pi/aW) \sim W$, that is, each boundary atom can support one highly localized low energy state. Their spectrum which can be derived from the dispersion of the ideal ribbon surface states is⁹ $E \sim t \exp(-kW)$ for $kW \gg 1$, where k is the wave vector deviation from the Dirac point. This spectrum provides the density of states which behaves as E^{-1} at $E \ll t/W$.

This extremely high low-energy density of states is obviously an artefact of our model and disappears if the hopping between next-nearest neighbors (NNN) on the graphene lattice is taken into account. It is characterized by the overlap integral t' which in graphene approximately equals to $0.2t$. In the following, we assume $t' > t/W$ which is the case for all graphene nanoribbons studied in the experiments. If the NNN overlap is taken into account, the edge states are hybridized and form a band of the width $\sim t'$. Thus, the (one-dimensional) density of states in the gap $|E| < t/W$ is approximately constant and equal to one state per surface atom per t' . Since the localization length is governed by the energy distance to the next subband, it is nearly independent of t' and still is approximately equal to W . We therefore coarse-grain over the ribbon elements of size $W \times W$ to obtain the low-energy level spacing within a coarse-grained element $\Delta E \sim t'/W$. Now, we can formulate the variable range hopping conductivity between these elements as

$$\sigma \sim e^{-\alpha n - t'/(nWT)}. \quad (4)$$

Optimizing over n , we find two regimes,

$$\sigma \sim \begin{cases} e^{-2\sqrt{\alpha t'/WT}} & \text{for } T < T_c \\ e^{-t'/(WT)} & \text{for } T_c < T < t/W \end{cases}, \quad (5)$$

with the crossover temperature $T_c = t'/W < t/W$. Again, higher-temperature (top line) and lower-temperature (bottom line) ranges correspond to VRH and NNH, respectively.

On the experimental side, Chen *et al.*¹¹ find that, *e.g.* in 20 nm wide GNR, which has a gap 28 mV, at relatively high temperatures, between 50 K and 100 K, transport is activated, $\sigma \propto e^{-E_g/T}$. The data is lacking at intermediate temperatures; however, the single low-temperature data point at 4 K shows conductivity much higher than would be expected from simple activated hopping. This may reflect a crossover from the nearest to variable range hopping. Our estimate for the crossover temperature is about 5 Kelvin, which is consistent with the experimental results. More detailed experimental data in the intermediate temperature regime should allow direct test of our predictions. It has also been found that the experimental size of the gap is smaller than t/W , which may be consistent with our value t'/W .

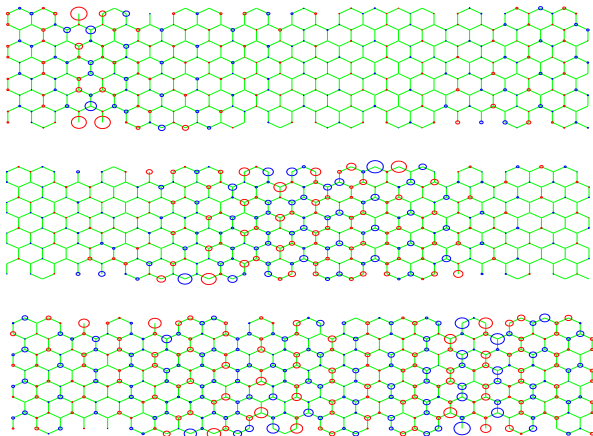


FIG. 3: Structure of the electronic wavefunctions in a strongly disordered zig-zag GNR. The disorder is generated by randomly eliminating half of carbon atoms at the edges of GNR. Periodic boundary conditions are applied in the horizontal direction. The energies of the states, from top down, $E = -0.071t$, $-0.089t$, $-0.255t$. Note how the confinement length increases away from the center of the band ($E = 0$). The typical confinement length at the energies inside the gap is of the order of the ribbon width.

IV. DISCUSSION AND CONCLUSIONS

The alternative explanation of experimental results was proposed in a model representing a GNR with *very strong* interface disorder as a chain of quantum dots, hosting localized electron states¹⁹. It was suggested by the authors that the experimentally observed gap has to do

with charging energy of the “quantum dots.” Indeed, recent experiments^{14,15} indicate that there are local charging centers in graphene nanoribbons. Compared to the case studied in Ref. 19, both cases that we considered above correspond to at most *mild* disorder. We therefore address now how the Coulomb interaction will affect our results.

The Coulomb interaction can modify low-temperature hopping conductivity. Interaction leads to opening of the soft Coulomb gap around the Fermi surface, which enters as an energy cost inversely proportional to the length of the hop¹⁷. Thus in the presence of the Coulomb interaction, the expression for conductivity has to be modified as

$$\sigma \sim e^{-\alpha n - t'/(nWT) - e^2/(e a_g WT)}. \quad (6)$$

Since $e^2/a_g t \sim 1$ in graphene, the Coulomb cost will become relevant if the dielectric constant of the embedding medium ϵ is smaller than $t/t' \sim 5$. While the functional form of conductivity in this case remains the same as in Eq. (5), the energy scale that defines the gap is different, $t'/W \rightarrow e^2/(\epsilon a_g W)$.

Thus, for freely suspended graphene the transport is in fact expected to be dominated by the *soft* Coulomb blockade. On the other hand, placing graphene in the vicinity of high- ϵ medium or metallic gate would reduce the Coulomb interaction strength and range²⁰, leading to crossover to Mott’s VRH.

Finally, we note that the $1/f$ noise observed by Chen *et al.*¹¹ may also be consistent with the scenario presented here, that is, it may be *intrinsic*, rather than caused by the charge fluctuations in the substrate, as was suggested in Ref. 11. Due to the presence of an exponentially broad distribution of the tunneling rates in the hopping transport, the experimentally observed Hooge relation²¹ between the low-frequency current noise and the DC current, $I_\omega^2/I^2 = A(\omega, T)/\omega$, can be naturally expected²². Straightforward application of the Shklovskii’s argument²² to one dimension leads to Hooge’s parameter $A \propto \exp(-BT)$ in the low-temperature (VRH) regime, and approximately constant A at high temperatures (NNH). Whether the $1/f$ noise is indeed intrinsic can be tested by varying the substrate properties, or performing measurement on a suspended GNR²³.

We acknowledge useful discussions with M. Fogler and A. F. Morpurgo. IM acknowledges the hospitality of Delft University of Technology, where part of this work was performed. This work was supported by EC FP6 funding (contract no. FP6-2004-IST-003673). Partial support was provided by US DOE.

¹ K. S. Novoselov, A. K. Geim, S. V. Morozov, D. Jiang, Y. Zhang, S. V. Dubonos, I. V. Grigorieva, and

A. A. Firsov, Science **306**, 666 (2004).

² A. K. Geim and K. S. Novoselov, Nature Materials **6**, 183

- (2007).
- ³ M. I. Katsnelson, K. S. Novoselov, and A. K. Geim, *Nature Physics* **2**, 620 (2006); V. V. Cheianov, V. Fal'ko, and B. L. Altshuler, *Science* **315**, 1252 (2007).
 - ⁴ H. Schomerus, *Phys. Rev. B* **76**, 045433 (2007); Ya. M. Blanter and I. Martin, *Phys. Rev. B* **76**, 155433 (2007).
 - ⁵ J. S. Bunch, Y. Yaish, M. Brink, K. Bolotin, and P. L. McEuen, *Nano Lett.* **5**, 287 (2005); L. A. Ponomarenko, F. Schedin, M. I. Katsnelson, R. Yang, E. W. Hill, K. S. Novoselov, and A. K. Geim, *Science* **320**, 356 (2008).
 - ⁶ M. Fujita, K. Wakabayashi, K. Nakada, and K. Kusakabe, *J. Phys. Soc. Japan* **65**, 1920 (1996); K. Nakada, M. Fujita, G. Dresselhaus, and M. S. Dresselhaus, *Phys. Rev. B* **54**, 17954 (1996).
 - ⁷ M. Ezawa, *Phys. Rev. B* **73**, 045432 (2006).
 - ⁸ A. H. Castro Neto, F. Guinea, and N. M. R. Peres, *Phys. Rev. B* **73**, 205408 (2006).
 - ⁹ L. Brey and H. A. Fertig, *Phys. Rev. B* **73**, 235411 (2006).
 - ¹⁰ V. Barone, O. Hod, and G. E. Scuseria, *Nano Lett.* **6**, 2748 (2006); Y.-W. Son, M. L. Cohen, and S. G. Louie, *Phys. Rev. Lett.* **97**, 216803 (2006).
 - ¹¹ Z. Chen, Y.-M. Lin, M. J. Rooks, and P. Avouris, *Physica E* **40**, 228 (2007).
 - ¹² M. Y. Han, B. Özyilmaz, Y. Zhang, and Ph. Kim, *Phys. Rev. Lett.* **98**, 206805 (2007).
 - ¹³ X. Li, X. Wang, L. Zhang, S. Lee, and H. Dai, *Science* **319**, 1229 (2008).
 - ¹⁴ C. Stampfer, J. Güttinger, S. Hellmüller, F. Molitor, K. Ensslin, and T. Ihn, *Phys. Rev. Lett.* **102**, 056403 (2009).
 - ¹⁵ X. Liu, J. B. Oostinga, A. F. Morpurgo, and L. M. K. Vandersypen, arXiv:0812.4038.
 - ¹⁶ N. F. Mott, *Metal-Insulator Transition* (Taylor & Francis, London, 1990)
 - ¹⁷ A. L. Efros and B. I. Shklovskii, in: *Electron-Electron Interactions in Disordered Systems*, eds. A. L. Efros and M. Pollak (North-Holland, Amsterdam, 1985) p. 409.
 - ¹⁸ M. E. Raikh and I. M. Ruzin, in: *Quantum Phenomena in Mesoscopic Systems*, eds. B. L. Altshuler, P. A. Lee and R. A. Webb (North Holland, Amsterdam, 1991) p. 301.
 - ¹⁹ F. Sols, F. Guinea, and A. H. Castro Neto, *Phys. Rev. Lett.* **99**, 166803 (2007).
 - ²⁰ Ya. M. Blanter and M. E. Raikh, *Phys. Rev. B* **63**, 075304 (2001).
 - ²¹ F. N. Hooge, *Physica (Amsterdam)* **60**, 130 (1972).
 - ²² B. I. Shklovskii, *Phys. Rev. B* **67**, 045201 (2003).
 - ²³ M. I. Katsnelson, K. S. Novoselov, T. J. Booth, S. Roth, J. C. Meyer, and A. K. Geim, *Nature* **446**, 60 (2007).